RESEARCH ARTICLE OPEN ACCESS

Bacterial Cellulose Nanocrystals from Low Cost Resources Reinforced Poly(ethylene oxide) Nanocomposites

B. Anwar(1,2), B. Bundjali(2) and I.M. Arcana(2)
[1] Department of Chemistry, Universitas Pendidikan Indonesia, Bandung, Indonesia
[2] Inorganic and Physical Chemistry Research Division, Institut Teknologi Bandung, Bandung, Indonesia
Corresponding Author: B. Anwar

ABSTRACT
This study investigated the effect of bacterial cellulose nanocrystals (BCNCs) derived from low cost resources as reinforcing nanofiller in poly(ethylene oxide) (PEO) based nanocomposites. The nanocrystals isolated from bacterial cellulose produced from the pineapple peel waste juice as a culture medium. TEM images showed that the morphology of BCNCs has a needle-like structure with an average length and diameter of 325 and 25 nm, respectively. The crystallinity index of BCNCs determined by XRD was 88%. The PEO/BCNCs nanocomposites were prepared by mixing the aqueous solution of PEO with the BCNCs suspension. The solid films were obtained by solution casting method. The morphology of nanocomposite films was characterized by SEM. The thermal and mechanical properties of nanocomposite films were characterized by DSC and tensile test, respectively. The incorporation of BCNCs into the PEO matrix change the morphology of both cross-section and surface films to be more regular and this lead the increasing in crystallinity and mechanical properties. However, the thermal properties of PEO matrix were decreased.

Keywords **–** bacterial cellulose nanocrystals, nanocomposites, poly(ethylene oxide), pineapple peel waste.

Date Of Submission: 10-01-2018 Date Of Acceptance: 03-02-2018

I. INTRODUCTION

The limited availability of non-renewable and unsustainable resources of material led researchers to develop renewable, sustainable, eco-friendly, biocompatible, and low-cost natural materials. Cellulose nanocrystals (CNCs) are one of the excellent nanomaterials that meet all of these criteria and is being currently developed [1]. CNCs was extracted from various sources of cellulose by removing the amorphous part. The use of bacterial cellulose (BC) as a cellulose source to obtain CNCs has some features, i.e. BC is a relatively pure cellulose source and its synthesis process can utilize various waste that pollutes the environment as a culture medium [2].

The CNCs were used mainly as a reinforcing nanofiller in a polymer matrix of a nanocomposite material. The reinforced polymer matrix may be rubber, polyolefin, polyurethane, polyester, starch, and protein [3]. One of them was as the reinforcing nanofiller on the polymer electrolyte membrane in the lithium ion battery. The most commonly used material for polymer electrolyte membrane was poly(ethylene oxide) (PEO) [4,5].

Samir et al [6] have studied the addition of CNCs derived from tunicin (a marine animal) into the PEO matrix. The results of this study indicate that the addition of tunicin CNCs causes a decrease in the degree of crystallinity and the melting point of the PEO matrix. However, the addition of filler causes thermal stabilization of the storage modulus for the composites above the melting point of the PEO matrix. Schroers et al [7] also reported that the addition of CNCs derived from tunicin into the poly(ethylene oxide co epichlorohydrin) copolymer matrix led to an increase in mechanical properties.

In the previous study, the CNCs have been isolated from bacterial cellulose (BC) produced by using pineapple peel waste juice as a culture medium [2]. In the present work, these low-cost bacterial cellulose nanocrystals (BCNCs) were used as the reinforcing nanofiller in PEO matrix. The morphology, as well as the thermal and mechanical properties were investigated.

II. MATERIALS AND METHODS

2.1 Materials

The chemicals used for the biosynthesis of BC and isolation of BCNCs were obtained from local suppliers with technical grade, whereas the chemicals used for analysis were purchased from Sigma and Aldrich Chemical Co. with pro analysis grade. The wild type strain of *Acetobacter xylinum* was obtained from local suppliers. Pineapple peel wastes were obtained from pineapple plantation in Subang, West Java, Indonesia. The molecular weight of poly(ethylene oxide) that used as a matrix was 600,000 g/mol.

2.2 Isolation of BCNCs

Isolation of BCNCs was including the processes of sulfuric acid hydrolysis, centrifugation, dialysis and sonication. The optimum conditions, according to the previous study [2], were a concentration of sulfuric acid of 50%, hydrolysis time of 25 minutes, temperature of 50°C and acid-BC ratio of 50 mL/g.

After hydrolysis, the sample was quenched by being poured out into a tenfold volume of deionized water. Cloudy part of cellulose dispersion was separated and then centrifuged at an acceleration of 4000 g for 10 minutes. Sediment was dialyzed against deionized water until the dispersion reached pH ~ 6, using CelluSep T4 Regenerated Cellulose Tubular Membrane MWCO 12.000–14.000. Finally, sonication was performed for 10 minutes using Branson 2510 Ultrasonic Cleaner. To obtain CNC powder, the suspension was freeze-dried using OPERON Freeze Dryer Bench Top FDB-5003.

2.3 Preparation of nanocomposites

A certain mass of PEO was dissolved in a certain volume of aqua DM and stirred using a hot plate and magnetic stirrer for 24 hours at room temperature. A certain volume of BCNCs suspension was poured into PEO solution and stirred again for 24 hours. In order to obtain the various BCNCs content in PEO matrix, the mass of PEO and BCNCs suspension volume that mixed were varied.

2.4 Characterization

2.4.1 Transmission electron microscopy (TEM)

Morphology and particle size distribution of BCNCs were observed by JEOL JEM–1400 Transmission Electron Microscope. A drop of dilute BCNCs suspension was deposited on carbon-coated microscope grids and allowed to dry for TEM imaging.

2.4.2 X-ray diffraction (XRD)

Diffractogram of BCNCs powders was obtained at room temperature by Philips PW 1835 diffractometer using CuKα radiation (λ = 1.54 Å) in the 2θ range of 5–90°. Potential difference and current use were 40 kV and 30 mA, consecutively. XRD analysis was conducted to investigate the polimorph structure and crystalinity index (CI). The empirical method was used to calculate the crystallinity index of cellulose [8] as shown in Eq. (1):

$$\mathrm{CI}(\%) = \frac{I_{200} - I_{am}}{I_{200}} \times 100 \qquad (1)$$

where I_{200} and I_{am} are the peak intensities of the crystalline and amorphous parts, respectively.

2.4.3 Scanning electron microscopy (SEM)

In order to investigate the morphology of nanocomposites, the dried film sample was coated by gold/palladium using ion sputter coater and observed by JEOL JSM–6560LA Scanning Electron Microscope with the operating voltage at 10 kV.

2.4.4 Differential scanning calorimetry (DSC)

Differential scanning calorimetry (DSC) was performed using a Simultaneous Thermal Analyzer (STA) Linseis PT1600. A certain mass of samples was placed in a sample pan of alumina. Each nanocomposite film sample was heated from 32 to 110 °C with a heating rate of 10 °C/min and a cooling rate of 30 °C/min. In the heating process, the melting point (T_m) taken from the peak of the melting endotherm and the enthalpy of fusion (ΔH_f^{obs}) was the peak area of the melting endotherm. In the cooling process, we obtained the crystallization temperature (T_c) and the enthalpy of crystallization (ΔH_c^{obs}) from the peak and the area of crystallization exotherm, respectively. The degree of crystallinity (X_C) could be determined from the data ΔH_f^{obs} using the following equation:

$$X_c(\%) = \frac{\Delta H_f^{obs}}{\Delta H_f^{o}} \times 100 \qquad (2)$$

where ΔH_f^0 = 197 J g^{-1} is the heat of fusion for 100% crystalline PEO [9].

2.4.5 Mechanical properties determination

The mechanical properties of polymers and its nanocomposites undergo tensile forces, such as modulus of elasticity, tensile strength, yield stress, elongation at break, and toughness were determined by the Textechno FAVIGRAPH tensile testing apparatus. The samples of 3 mm width and a certain thickness were applied a certain force at a rate of 6.0 mm/min, then the data on their mechanical properties and their stress-strain curves were recorded.

III. RESULTS AND DISCUSSION

3.1 Morphology and particle size of BCNCs

The length and diameter distribution of BCNCs were estimated from TEM image, which is obtained by measuring the 200 individual particles using the ImageJ software. As shown in Fig. 1, the CNCs have a needle-like structure with an average length and diameter of 325 nm and 25 nm, respectively, and an average aspect ratio (L/D) of around 13.

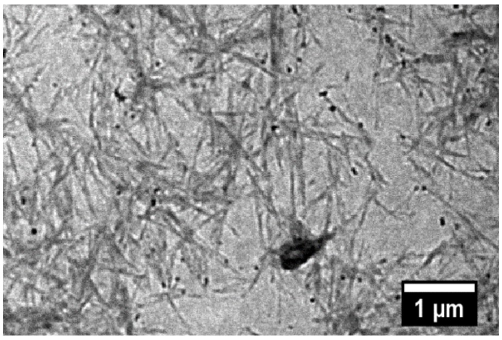

Figure 1. Transmission electron micrograph of BCNCs

3.2 Polymorph structure and crystallinity index of BCNCs

The results of XRD measurement give the information about the polymorph structure and crystallinity of cellulose. The BCNCs provide a diffraction peak at 2θ = 14.7°, 17.0° and 22.7° associated with crystallographic planes (1-10), (110) and (200). These diffraction peaks are typical to the polymorph structure of crystalline cellulose I (Fig. 2).

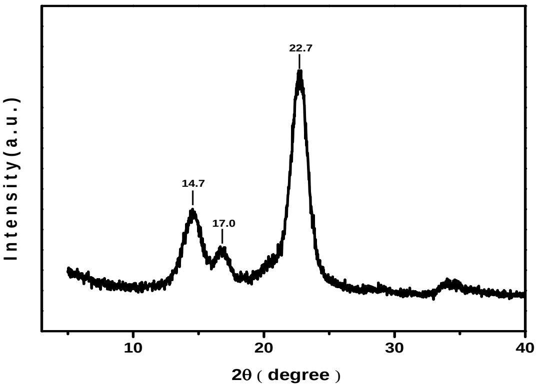

Figure 2. Diffractogram of BCNCs

The crystallinity index (CI) was calculated using Eq. (1). The maximum intensity (I_{200}) is at 2θ = 22.7° and the lowest intensity (I_{am}) is at 2θ = 18.2° for cellulose I [10]. The crystallinity index of BCNCs determined by this method was 88%.

3.3 Morphology of nanocomposite film

The morphology of nanocomposite films was characterized by SEM. Fig. 3 shows the SEM images for cross-sections of PEO matrix and PEO/BCNCs nanocomposite films, whereas the SEM images of their surface morphology were shown in Fig. 4.

The morphology of the cross-section of the PEO matrix film was irregular and shows the fibrillar region and holes (Fig. 3a). The fibrillar form is caused due to the semi-crystalline nature of PEO and the appearance of holes could result from entrapped air within the film during evaporation of the water solvent [6]. The cross-sectional morphology of the PEO/BCNCs nanocomposite film exhibit more regularly than the PEO matrix (Fig. 3b). More regular morphology is associated with higher degrees of crystallinity.

The indication of presence of BCNCs in the PEO matrix was not clearly observed, this is because the amount of BCNCs was measly. However, not all individual particles of BCNCs were evenly distributed in the PEO matrix, but some form a small aggregate (Fig. 4b).

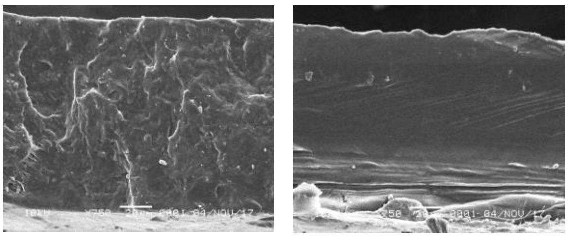
(a) (b)

Figure 3. Scanning electron micrographs from the cross-sectional of (a) unfilled PEO matrix and (b) nanocompostes filled with 5 wt% BCNCs

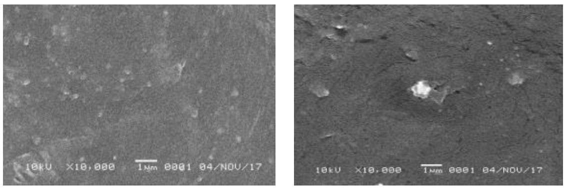

(a) (b)

Figure 4. Scanning electron micrographs from the surface of (a) unfilled PEO matrix and (b) nanocompostes filled with 5 wt% BCNCs

3.4 Thermal properties of nanocomposites

The DSC measurements were performed on heating and cooling processes. In the heating process the melting point (T_m) and the enthalpy of fusion (ΔH_f^{obs}) were obtained. Whereas from the cooling process, the temperature crystallization (T_c) and the enthalpy of crystallization (ΔH_c^{obs}) were acquired.

The degree of crystallinity (X_C) of the films was determined from the enthalpy of fusion data (ΔH_f^{obs}) by using Eq. (2). In addition, the degree of crystallinity per gram of PEO matrix (X_P) could also determine by dividing X_C by the mass of the PEO matrix in the composite. The thermal parameters and the degree of crystallinity of the nanocomposite films were given in Table 1.

The incorporation of BCNCs into the PEO matrix effect the increasing of the crystallinity degree of the film. According to Samir et al [6], cellulose can interact significantly with both water and the PEO. However, cellulose-water interactions were stronger than cellulose-PEO interactions. This cellulose-water interactions was allegedly lead the increasing of the crystallinity degree of the nanocomposite films. In the water evaporation step, the presence of BCNCs that interact strongly with water will cause the water evaporation to take place more slowly, so that the polymer chains have time to organize themselves and configure a more crystalline solid.

Table 1. Thermal properties and degree of crystallinity of BCNCs filled PEO using data obtained from the DSC curves

BCNCs content (wt%)	ΔH_f^{obs} (J/g)	T_M (°C)	ΔH_C^{obs} (J/g)	T_C (°C)	X_C (%)	X_P
0	63,89	81,9	62,21	55,6	32,4	32,4
2,5	80,66	81,5	59,39	46,4	40,9	41,9
5	78,76	79,1	56,61	48,9	40,0	42,1

The decrease in melting point (T_M) due to the incorporation of BCNCs could be ascribed to the strong interaction between oxygen ethers of PEO and hydroxyl groups (–OH) of BCNCs [11]. In addition, the incorporation of BCNCs into the PEO matrix also decreases the crystallization temperature (T_C) that caused by the anti-nucleation effect of BCNCs. Theoretically, the rate of nucleation is the product of mass transport and the nucleation parameters. The mass transport factor is related to the self-diffusion of the polymer chain. The strong affinity of PEO molecules toward the reactive cellulose surfaces results in a restricted mobility of PEO molecules that connected to the surface of BCNCs. In addition, the increased viscosity of polymer melts due to incorporation of BCNCs will increase the activation energy of polymer chain diffusion.

3.5 Mechanical properties of nanocomposites

The mechanical properties testing of nanocomposite films was performed by using a tensile test apparatus conducted at room temperature. All film samples initially show an elastic deformation region. The stress-strain curves for PEO matrix and nanocomposite film show a peak over a period of elastic deformation (yield stress) and then the stress drops to zero. The results of mechanical properties testing of nanocomposite films on various BCNCs contents were shown in Table 2.

The incorporation of BCNCs to the PEO matrix increases the modulus of elasticity, tensile strength, and stiffness. The tensile strength and the optimal yield point were obtained at the BCNCs content of 2.5 wt%. This reinforcement effect was caused by an increase in the degree of crystallinity due to the incorporation of BCNCs into the PEO matrix. In addition, the hydrogen bonds that occur between BCNCs and PEO matrix result more rigid materials. Fig. 5 shows the mechanical behavior of nanocomposite films on various BCNCs contents.

Table 2. Mechanical properties of PEO/BCNCs nanocomposites

BCNCs content (wt %)	Modulus of elasticity (MPa)	Tensile strength (MPa)	Yield stress (MPa)	Elongation at break (%)
0	190	11,8	11,8	1086
2,5	201	12,9	12,9	83
5,0	206	12,5	12,5	730

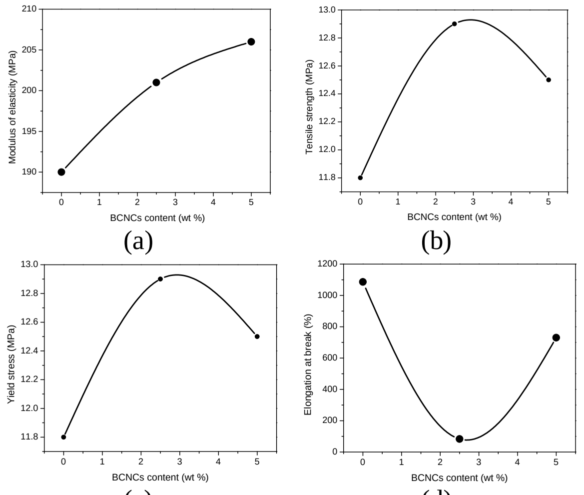

(a) (b)

(c) (d)

Figure 5. Mechanical behaviors of nanocomposites film on various BCNCs contents, (a) modulus of elasticity, (b) tensile strength, (c) yield stress, and (d) elongation at break

IV. CONCLUSION

Nanocomposite materials were prepared from an aqueous suspension of low cost bacterial cellulose nanocrystals (BCNCs) and an aqueous solution of poly(ethylene oxide) (PEO). The BCNCs have a needle-like structure with sufficient aspect ratio and high crytallinity index. The incorporation of BCNCs into PEO matrix caused the increasing the degree of crystallinity and induce the increasing of mechanical properties of the nanocomposites. The optimum BCNCs content which provides maximum reinforcement was 2.5 wt%. In accordance with previous research, the incorporation of BCNCs caused the decreasing of melting point and crystallization temperature of PEO matrix. In the near future study, the nanocomposite will be used as a polymer electrolyte membrane for lithium ion battery.

ACKNOWLEDGEMENTS

This work has supported by the Research Grant of Competition Research Program under the Directorate of Higher Education, the Ministry for Research, Technology, and High Education, the Republic of Indonesia, and also the Institute for Research – LPPM, Institut Teknologi Bandung (ITB).

REFERENCES

[1]. B.L. Peng, N. Dhar, H.L. Liu, and K.C. Tam, Chemistry and application of nanocrystalline cellulose and its derivatives: A nanotechnology perspective, *The Canadian Journal of Chemical Engineering, 9999,* 2011, 1–16.

[2]. B. Anwar, B. Bundjali, and I.M. Arcana, Isolation of cellulose nanocrystals from bacterial cellulose produced from pineapple peel waste juice as a culture medium, *Procedia Chemistry, 16*, 2015, 279–284 .

[3]. J. Huang, P.R. Chang, and A. Dufresne, Polysaccharide nanocrystals: Current status and prospect in material science, in J. Huang, P.R. Chang, N. Lin, and A. Dufresne (Eds), *Polysaccharide-based nanocrystals chemistry and applications,* (Weinheim-Germany: Wiley-VCH Verlag GmbH & Co., 2015) 1–13.

[4]. F. Croce, G.B. Appetecchi, L. Persi., and B. Scrosati, Nanocomposite polymer electrolytes for lithium batteries, *Nature, 394*, 1998, 456–458.

[5]. J. McBreen, H.S. Lee, X.Q. Yang, and X. Sun, New approaches to the design of polymer and liquid electrolytes for lithium batteries, *Journal of Power Sources, 89*, 2000, 163–167.

[6]. M.A.S.A. Samir, F. Alloin, J-Y. Sanchez, and A. Dufresne, Cellulose nanocrystals reinforced poly(oxyethylene), *Polymer, 45*, 2004, 4149–4157.

[7]. M. Schroers, A. Kokil, and C. Weder, Solid polymer electrolytes based on nanocomposites of ethylene oxide–epichlorohydrin copolymers and cellulose whiskers, *Journal of Applied Polymer Science, 93,* 2004, 2883–2888.

[8]. L. Segal, J.J. Creely, A. Martin, and C. Conrad, An empirical method for estimating the degree of crystallinity of native cellulose using the X-ray diffractometer, *Textile Research Journal, 29*, 1959, 786–794.

[9]. Y. Gnanou and M. Fontanille, *Organic and physical chemistry of polymers* (Hoboken: John Wiley & Sons, Inc., 2008).

[10]. M.L. Nelson and R.T. O'Connor, Relation of certain infrared bands to cellulose crystallinity and crystal lattice type. Part II. A new infrared ratio for estimation of crystallinity in celluloses I and II, *Journal of Applied Polymer Science, 8*, 1964, 1325–1341.

[11]. T. Kondo and C. Sawatari, Intermolecular hydrogen bonding in cellulose/poly(ethylene oxide) blends: thermodynamic examination using 2,3-di-*O*- and 6-*O*-methylcelluloses as cellulose model compounds, *Polymer, 35(20)*, 1994, 4423–4428.

*B. Anwar. "Bacterial Cellulose Nanocrystals from Low Cost Resources Reinforced Poly (ethylene oxide) Nanocomposites." International Journal Of Engineering Research And Applications (IJERA), vol. 08, no. 01, 2018, pp. 01–05.